Electronic supplementary Information for

p-MoS_2/*n*-InSe van der Waals heterojunctions and their applications in all-2D optoelectronic devices

Pan Li, Kai Yuan, Der-Yuh Lin, Tingting Wang, Wanying Du, Zhongming Wei, Kenji Watanabe, Takashi Taniguchi, Yu Ye* and Lun Dai*

* To whom correspondence should be addressed. E-mail: ye_yu@pku.edu.cn, lundai@pku.edu.cn

S1. The electron mobility (μ_e) and concentration (n_{2D}) of InSe nanoflake.

The electron mobility of the InSe nanoflake (μ_e) can be estimated from the channel transconductance (g_m) of the FET, which is expressed as: $\mu_e = g_m\left[\frac{L^2}{(C_g V_{ds})}\right]$, and $g_m = \frac{\partial I_{ds}}{\partial V_g}$, where L is the channel length, C_g is the gate capacitance. The C_g can be expressed as: $C_g = \varepsilon\varepsilon_0 L \cdot \frac{W}{h}$, where ε and h are the dielectric constant and thickness of SiO_2, and W is the channel width. The g_m was obtained to be 3.6 μA/V by fitting the liner part of the I_{ds} versus V_{gs} curve of the InSe FET (Fig. 2b) at V_{ds} = 0.5 V, C_g is 8.68×10^{-16} F at L =1.85 μm, W =3.86 μm, h =285 nm. Thus, we obtain an electron mobility (μ_e) of about 285 $cm^2/V\cdot s$. Electron concentration (n_{2D}) can be estimated from the expression: $n_{2D} = \frac{L \quad 1}{WR\mu_e q}$, where R and q are channel resistance and electron charge, respectively. According to the I_{ds} vs V_{ds} curves (Fig. 2a in manuscript), at V_{gs}= 30 V, and 40 V when the channel was turned on, we obtain n_{2D} = 2.19×10^{12} cm^{-2}, and 3.32×10^{12} cm^{-2}, respectively.

S2. The hole mobility (μ_h) and concentration (p_{2D}) of MoS_2 nanoflake

The hole mobility (μ_h) of MoS_2 nanoflake can be estimated from the channel transconductance (g_m) of the FET, which is expressed as: $\mu_h = g_m\left[\frac{L^2}{(C_g V_{ds})}\right]$, and $g_m = \frac{\partial I_{ds}}{\partial V_g}$, where L is the channel length, C_g is the gate capacitance. The C_g can be expressed as: $C_g = \varepsilon\varepsilon_0 L \cdot \frac{W}{h}$, where ε and h is the dielectric constant and thickness of SiO_2, W is the channel width respectively. The g_m was obtained to be 52 nA/V by fitting the liner part of the I_{ds} versus V_{gs} curve of the MoS_2 FET (Fig. 2d) at V_{ds} = 0.5 V, C_g is 2.16×10^{-15} F at L =1.9 μm, W =9.4 μm, h =285 nm. Thus, we obtained hole mobility (μ_h) of about 1.7 $cm^2/V\cdot s$. Hole concentration (p_{2D}) can be estimated from the expression: $p_{2D} = \frac{L \quad 1}{WR\mu_h q}$, where R and q are channel resistance and electron charge, respectively. According to the I_{ds} vs V_{ds} curves at zero back gate (Fig. 2c in the manuscript), we obtain $p_{2D} = 3.03\times10^{13}$ cm^{-2}.

S3. Comparison of *h*BN encapsulated and non-encapsulated InSe samples.

The encapsulated InSe FET shows negligible hysteresis loop in the transfer curves. However, the non-encapsulated InSe FET shows larger hysteresis loop in the transfer curves (Fig. S1), because of the molecules absorption/desorption at the exposed surfaces. The highest on-current achieved under 40 V back gate is about 1 μA, which is two to three orders of magnitude smaller than that of encapsulated sample at same V_{ds} and V_g.

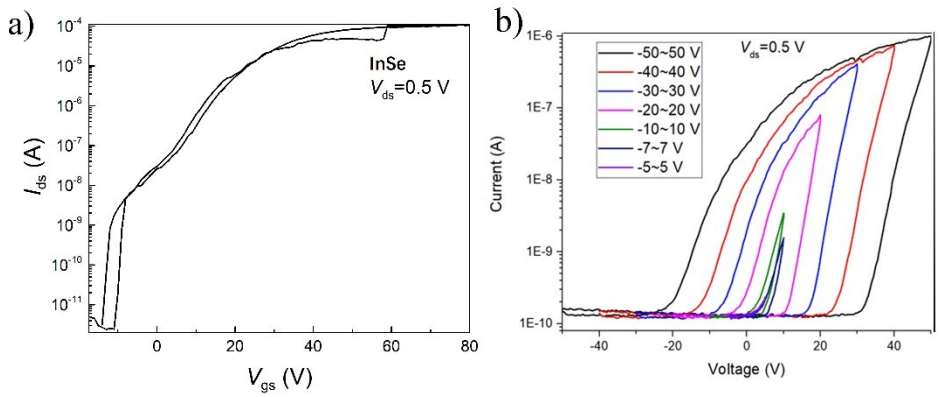

Fig. S1 The I_{ds} vs. V_{gs} curves for an encapsulated (Fig. S1a) and a non-encapsulated (Fig. S1b) InSe FET under different V_{gs} scanning ranges with V_{ds} = 0.5 V.

S4. Determination of the MoS_2/InSe band alignment

The determination of MoS_2/InSe band alignment is based on the reported bandgaps, affinities, and measured work functions of MoS_2/InSe nanoflakes. The reported bandgap value of few-layer MoS_2 is1.28 eV,[S1, S2] and that of few-layer InSe is 1.22 eV in accordance with our photoluminescence measurement of the InSe nanoflake (Fig. S2). The reported affinity values of MoS_2 and InSe are 4.0 eV[S3, S4] and 4.05 eV,[S4] respectively. The work functions of MoS_2 and InSe are calculated to be 5.31 eV and 4.2 eV, respectively, based on the measured carrier concentrations and reported band structures, by using the following equations:

$n = n_i e^{(E_F - E_i)/\kappa_B T}$, $p = n_i e^{(E_i - E_F)/\kappa_B T}$, $n_i^2 = N_c N_v e^{-\frac{E_c - E_v}{\kappa_B T}}$, where n and p are the carrier concentrations, n_i is the intrinsic carrier concentration; N_c and N_v are the equivalent density of states of conduction and valence bands, respectively; κ_B is the boltzmann's constant. N_c and N_v can be expressed as: $N_c = 2(\frac{2\pi m_n \kappa_B T}{h^2})^{3/2}$, $N_v = 2(\frac{2\pi m_p \kappa_B T}{h^2})^{3/2}$, respectively; where m_n and m_p are the effective masses of electron and hole, respectively. With that, the MoS_2/InSe forms a type-II

heterostructure with a barrier between the conduction bands and the valence bands of about 1.16 eV and 1.10 eV, respectively.

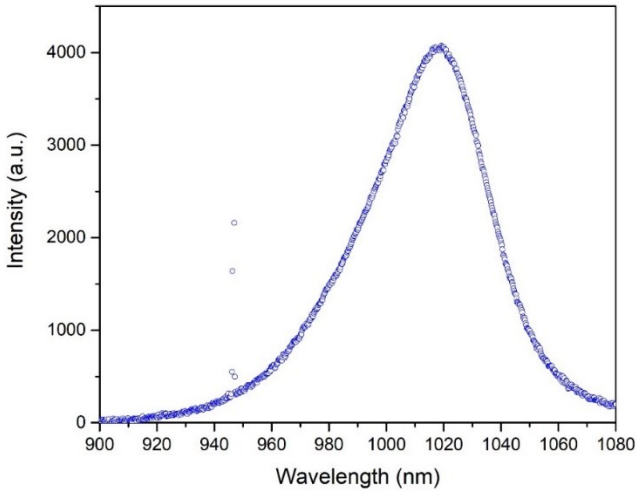

Fig. S2 Photoluminescence spectrum of the InSe nanoflake with a single emission peak centered at ~1020 nm.

S5. Size information of the flakes and heterostructure.

Before stacking the van der Waals heterostructure, we firstly exfoliated the few-layer InSe and MoS_2 flakes onto the Si/SiO_2 substrates. The thicknesses of the flakes were roughly obtained under the microscope, due to interference from the cavity formed between the flake and substrate interfaces.[S5, S6] In this device, we used a top layer *h*BN of ~10 nm, bottom layer *h*BN of ~30 nm, MoS_2 flake of 10-15 nm, and InSe flake of 10-15 nm, selected through the optical contrast (Fig. S3a-c). After the full assembly of the heterostructure, we conducted the AFM measurements to identify the precise thickness of each layer (Fig. S3e). For one of our heterostructures, the area of the heterostructure was measured to be ~51 μm^2 from the optical image (Fig. S3d). The thicknesses of the MoS_2 and InSe flakes were measured to be 13 nm and 15 nm, respectively.

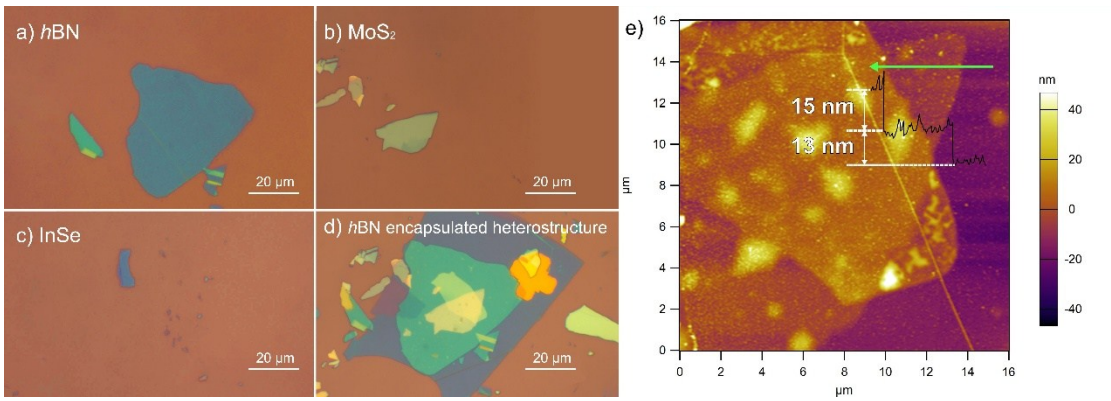

Fig. S3: (a-d) The optical images of the bottom *h*BN layer, MoS_2 flake, InSe flake, and fully stacked heterostructure. (e) The AFM height image of stacked heterostructure. The green arrow represents the measured thickness of MoS_2 and InSe flakes of 13 nm and 15 nm, respectively.

S6. Dry transfer method.

A piece of adhesive tape with a hole in the center was first adhered to a silicon chip. Subsequently, the silicon chip was coated with polypropylene carbonate (PPC, Sigma-Aldrich, CAS 25511-85-7) at 2000 rpm. The tape with a PPC thin film was manually peeled from the silicon substrate and placed onto a transparent elastomer stamp (polydimethylsiloxane, PDMS). The stamp was then affixed to a glass slide, which was attached to a micromanipulator with the PPC film side down.

Then, the transfer processes are shown in Fig. S4. First, PPC slowly wraps the entire sample from one side of the sample at 40 ℃, then we picked up the previously exfoliated top-*h*BN and MoS_2 flake in sequence from Si/SiO_2 substrate by PPC at room temperature (Fig. S4a, b). 1 min 90 ℃ anneal of the glass slide with the stamp and sample on top after each pick-up process is necessary to make the sample smooth. To avoid the degradation of InSe, the InSe related exfoliation and transfer processes were done in a glove box (O_2, H_2O < 0.1 ppm) (Fig. S4c-e). The selected InSe nanoflake was picked up by the previously picked top-*h*BN/MoS_2 heterostructure on PPC (Fig. S4c) and transferred onto another *h*BN nanoflake on Si/SiO_2 substrate (Fig. S4d). The *h*BN encapsulated heterostructure was detached from PDMS/PPC at 60 °C and left on the device substrate (Fig. S4e).

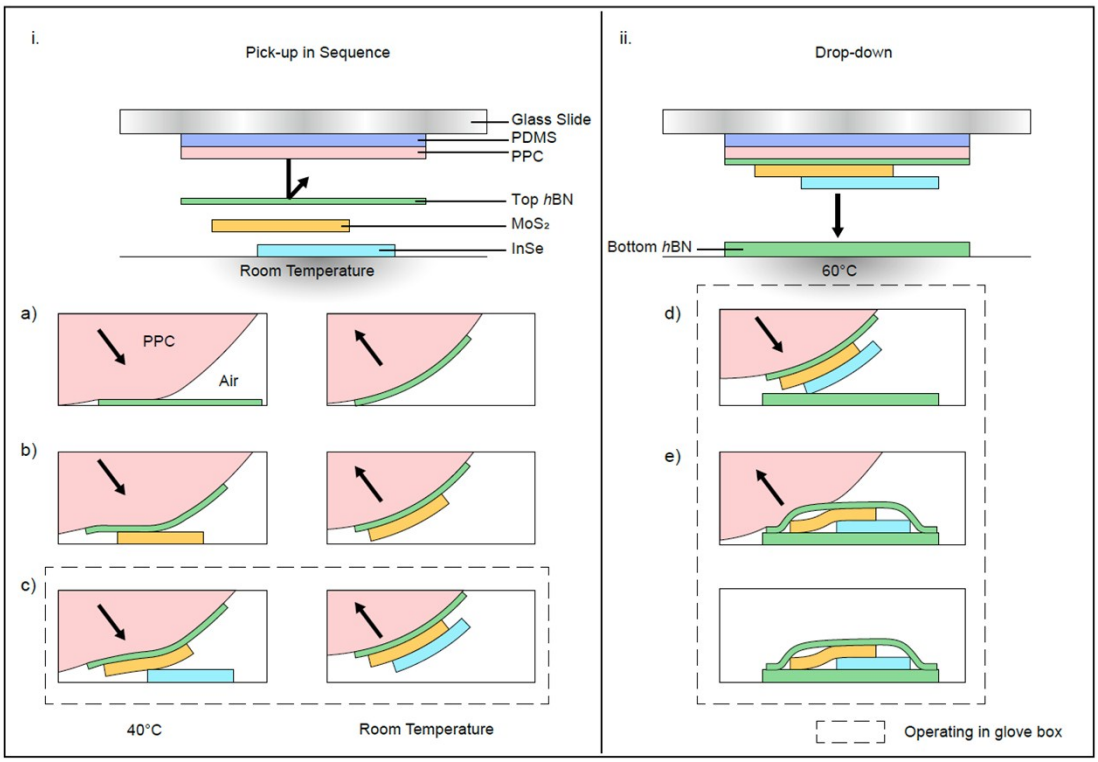

Fig. S4: The schematic diagram for the dry transfer method. (i) Picking the top-*h*BN/MoS_2/InSe flakes in sequence from Si/SiO_2 substrate by PPC. (ii) Putting the PPC with top-*h*BN/MoS_2/InSe heterostructure facing down onto the bottom-*h*BN on Si/SiO_2 substrate. Then PPC was lifted off slowly. Finally, the *h*BN encapsulated heterostructure was left on the device substrate.

References:

S1 S. Han, H. Kwon, S. K. Kim, S. Ryu, W. S. Yun, D. Kim, J. Hwang, J.-S. Kang, J. Baik and H. Shin, *Physical Review B*, 2011, **84**, 045409.

S2 H. Li, J. Wu, Z. Yin and H. Zhang, *Accounts of chemical research*, 2014, **47**, 1067-1075.

S3 S. Das, H.-Y. Chen, A. V. Penumatcha and J. Appenzeller, *Nano Lett.*, 2012, **13**, 100-105.

S4 W. Feng, X. Zhou, W. Q. Tian, W. Zheng and P. Hu, *Physical Chemistry Chemical Physics*, 2015, **17**, 3653-3658.

S5. K. Novoselov, D. Jiang, F. Schedin, T. Booth, V. Khotkevich, S. Morozov and A. Geim, *Proceedings of the National Academy of Sciences of the United States of America,* 2005, **102**, 10451-104

S6. H. Li, Z. Yin, Q. He, H. Li, X. Huang, G. Lu, D. W. H. Fam, A. I. Y. Tok, Q. Zhang

and H. Zhang, *small,* 2012, **8**, 63-67.